Int. J. Electrochem. Sci., 7 **(2012)** 7376 - 7389

International Journal of
ELECTROCHEMICAL
SCIENCE
www.electrochemsci.org

Stress Corrosion Behaviors of Steel Wires in Coalmine under Different Corrosive Mediums

S. Q. Wang[1], *D. K. Zhang*[2,*], *D. G. Wang*[1], *L. M. Xu*[1], *S. R. Ge*[1]

[1] School of Mechatronic Engineering, China University of Mining and Technology, Xuzhou 221116)
[2] School of Materials Science and Engineering, China University of Mining and Technology, Xuzhou 221116)
[*]E-mail: dkzhang@cumt.edu.cn

Received: 27 June 2012 / *Accepted:* 19 July 2012 / *Published:* 1 August 2012

This paper investigates stress corrosion behaviors of steel wires in coalmine under different polarization potential and different corrosive mediums simulated mine trickling water by using slow strain rate tests (SSRT). Stress corrosion cracking (SCC) mechanisms of steel wires were explored by comparisons of their mechanical properties, fracture morphology analysis and scanning polarization curve. The results show that steel wires under different corrosive mediums all present stress corrosion cracking (SCC) phenomenon, and the SCC susceptibility is the strongest in neutral solution. When applying strong anodic polarization potential, steel wires in acidic solution don't exhibit SCC phenomenon, while SCC in neutral and alkaline solution is controlled by anodic dissolution. With the decreasing of applied anodic potential, the SCC mechanism in alkaline solution is controlled by anodic dissolution and hydrogen embrittlement. In the self-corrosion area, SCC mechanisms of steel wires are all controlled by anodic dissolution and hydrogen embrittlement in three corrosive solutions with stronger SCC susceptibility. When the cathodic polarization potential is applied, SCC mechanisms under three corrosive mediums are mainly controlled by hydrogen embrittlement, and strong hydrogen evolution reaction enhances the SCC susceptibility.

Keywords: steel wire; stress corrosion; polarization potential; hydrogen embrittlement

1. INTRODUCTION

Steel wire rope is an important component of hoisting system in coalmine. The rope performance not only has a direct impact on coal mine production, but also is related to the security of

personnel life. It has proved that working conditions of wire rope in coalmine affect the service life of hoisting rope greatly. The wire rope is always used in the bad environments of high wind speed, large humidity and much trickling water and thereby harmful ions can make the rope surface corroded. The data shows rust can induce more than 30% strength loss of steel wires and even as high as 50%. In addition, wire rope as the transport equipment is subjected to high applied stress in the service process, and the combination of high stress and corrosion can produce dangerous low stress failure forms and even stress corrosion cracking of steel wire. The phenomenon occurs suddenly without obvious warning, which is the most destructive form of damage.

In the study of stress corrosion behaviors, many researchers have proposed a variety of stress corrosion cracking (SCC) mechanisms [1-9], among which the anodic dissolution theory and hydrogen brittlement theory are most accepted SCC mechanism [10]. In recent years, lots of researches on stress corrosion behaviors of metal materials have been carried out [11-20]. Liu zhi-yong et al [21, 22] studied SCC issues of pipeline steel in acidic soil. Parkins et al [23-28] studied SCC mechanisms of nearly neutral solution (NS_4) and high pH solution (Na_2CO_3 and $NaHCO_3$). Huang Yan-liang et al [29] explored SCC mechanisms of stainless steel in acid chloride solution. Ruther et al [30] found the sensitization of 304 stainless steel occurred intergranular stress corrosion easily in high temperature oxygen water with pH value of 6. Berge et al [31] studied the shortest time of 316 stainless steel producing 500μm crack in NaOH solution at 350 centigrade. The results showed that crack initiation time decreased when the quality concentration of NaOH solution increased from 40 $g \cdot L^{-1}$ to 50 $g \cdot L^{-1}$.

At present, there are few researches on stress corrosion of steel wires in certain trickling water environment. In the background of stress corrosion accident of steel wire in coalmine, the stress corrosion behaviors of high strength steel wire under different corrosive mediums with three different pH values simulated mine trickling water were performed in this paper. Slow strain tensile test (SSRT) of smooth wire without gap was applied to study stress corrosion behaviors of steel wire in simulated trickling water. The electrochemical method was used to study the effects of different polarization potentials on stress corrosion cracking (SCC) sensitivity. In addition, the stress corrosion cracking (SCC) mechanisms of steel wires were explored by comparisons of their mechanical properties, fracture morphology analysis and scanning polarization curves.

2. EXPERIMENTAL

All specimens are high strength steel wires with the diameter of 1mm, and their chemical composition is shown in table 1. The gauge length of steel wire is 150mm, which was always submerged in the corrosion solution. According to composition of mine trickling water in China, the composition of corrosive solutions with three pH values simulated mine trickling water are shown in table 2.

Table 1. Chemical composition of wire specimens (wt %)

Composition	Fe	Mn	Si	Zn	Ni	C	S	P
Percentage	94.62	0.39	0.02	4.53	0.01	0.84	0.001	< 0.001

Table 2. Typical water quality of coalmine in China

pH value	Content of ions / mg/L							
	K^+	Na^+	Ca^{2+}	Mg^{2+}	Cl^-	SO_4^{2-}	HCO_3^-	D_0
2.97	11.73	92.42	676.55	364.74	28.36	3283.81	18.92	5.60
6.97	11.73	141.16	80.56	49.33	89.33	551.38		5.60
9.97	11.73	35.63	54.43	36.45	89.33	232.95		5.60

All slow strain rate tests (SSRT) were performed at the strain rate of 10^{-6} on constant strain rate testing machine. Tensile specimens were exerted different applied polarization potentials by CS electrochemical workstation (E_{corr}+ΔE). Parameters of E_{corr} and ΔE are the open circuit potential and relatively E_{corr} potential, respectively. ΔE were -500 mV and -250 mV, respectively in the case of cathodic polarization as compared to 200 mV and 400 mV in the case of anodic polarization. In addition, ΔE was 0 mV in the condition of self-corrosion. The saturated calomel electrode was used as reference electrode, platinum wire as the counter electrode, and steel wire as the working electrode. Before the tensile test, specimens were pre-soaked for 24h. After SSRT, fractured specimens were washed by ultrasonic wave, and then their reduction of areas were measured. Circumferential surfaces and fracture morphologies of fracture specimens were observed using scanning electron microscopy (SEM), and then the effects of different solutions and applied potentials on stress corrosion behavior of steel wire were analyzed.

In order to further study SCC mechanisms of steel wires under three corrosive mediums and the effects of different polarization potential on SCC behaviors, the polarization curves were obtained with the fast scanning rate of 50 mV/s and with the slow scanning rate of 0.5 mV/s. The potentials were all related to the saturated calomel electrode.

3. RESULTS AND DISCUSSION

3.1 Tensile curve analysis

Figure 1 shows the stress-strain curves of steel wire under different polarization potentials in three corrosive mediums. As compared to tensile curves in air, tensile strengths in three solutions are

all found to be significantly lower than those in air, and uniform percentage elongation reduced to different extents, which indicates certain SCC susceptibility under different corrosive mediums.

Figure 2 shows the effects of different applied polarization potentials on variation curves of steel wire current density, tensile strength and uniform percentage elongation in three corrosive solutions. The algorithm of uniform percentage elongation is shown in Fig 1(a) with the starting point selected from the start of flexibility deformation. When applying anodic potential, the variation trend of wire current density is similar in three corrosive solutions, i.e. current density decreases rapidly with the decreasing of applied potential. The descent rate is the largest in acidic solution as compared to the smallest rate in alkaline solution. When applying cathodic potential, wire current density reduces slowly with the decreasing of applied potential. In neutral solution, the variation trends of tensile strength and uniform percentage elongation are the same. When the anodic potential is applied, they first decreases and then increases with the decreasing of potential, whereas the decrease of potential results in their gradual decrease when applying the cathodic potential.

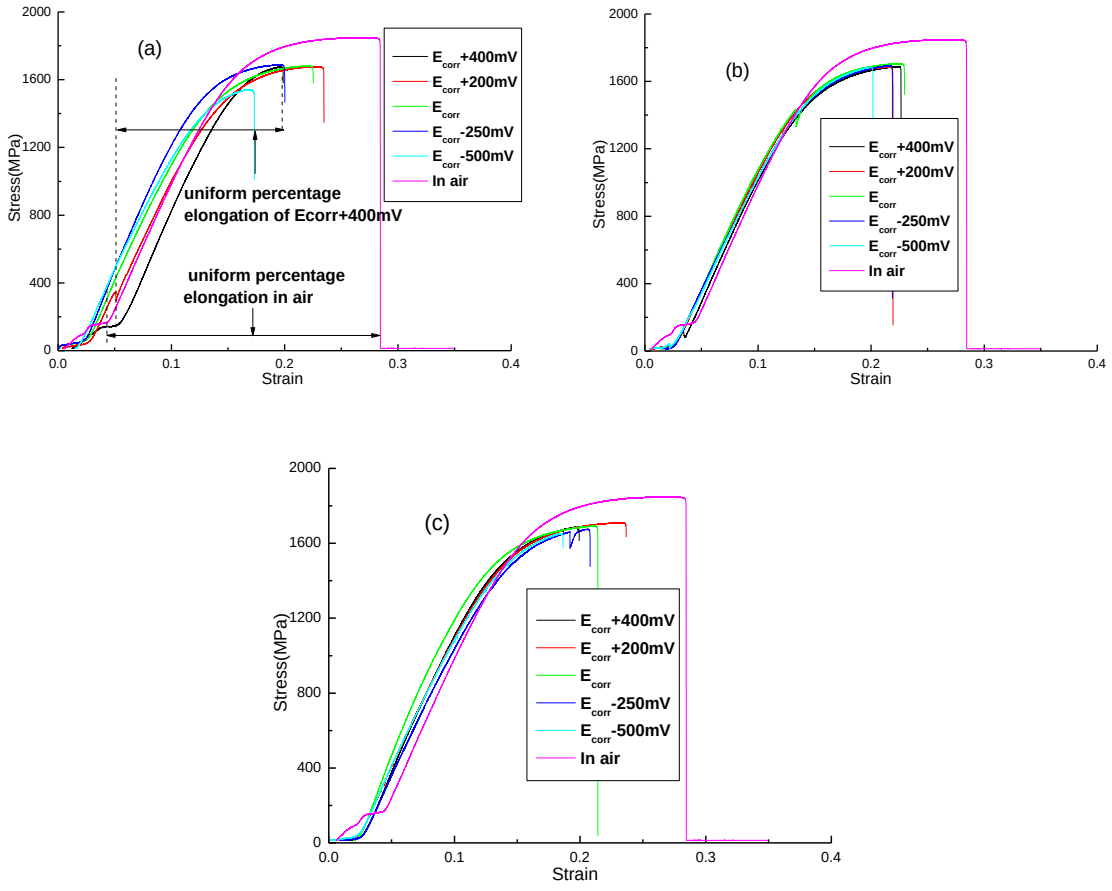

Figure 1. Stress-strain curves of steel wires in three kinds of corrosive mediums(a) acidic solution; (b) neutral solution; (c) alkaline solution

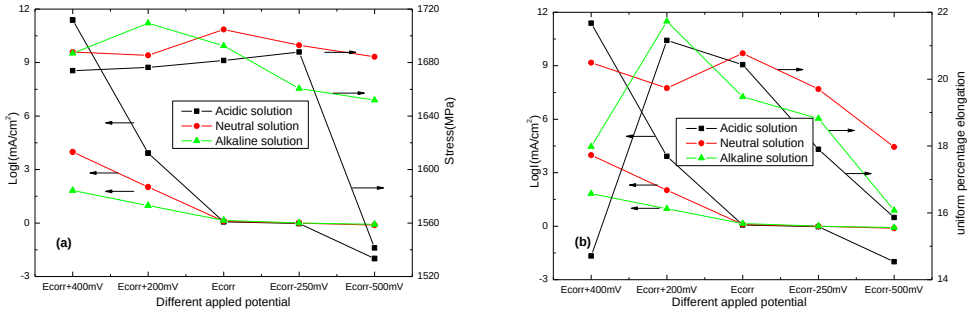

Figure 2. Variation curves of wire current density, tensile strength and uniform percentage elongation under different applied polarization potentials in three corrosive solutions. (a) variation curve of current density vs tensile strength; (b) variation curve of current density vs uniform percentage elongation

In the same corrosive solution, variation trend of wire tensile strength is not obvious. When the applied E_{corr} is -400 mV in acidic solution, the tensile strength reduces to 1541.4MPa. That's because there are lots of hydrogen ions which accelerate hydrogen evolution reaction and enhance SCC susceptibility and thereby increase the fragility. Variation trend of wire uniform percentage elongation in acidic solution is similar to that in alkaline solution. From the applied potential E_{corr} of +200 mV, uniform percentage elongation gradually decreases with the decrease in applied potential.

3.2 Reduction of area analysis

Figure 3 shows the reduction of area of steel wires under different applied polarization potentials in three corrosive solutions. In order to characterize materials SCC susceptibility in the corrosive solution, $I_\psi = (1-\psi_E/\psi_O) \times 100\%$ is defined as the ratio of reduction-in-area by Liu etc. [21, 32], which is used to describe material toughness loss. Parameters of ψ_E and ψ_O are the reduction of area in mediums and air, respectively. They thought SCC susceptibility increased with the increasing of I_ψ.

However, it can be seen from Fig.3 that especially in acidic solution, the larger applied polarization potential induces severe anodic dissolution of wire surface and thinned sample, which causes decreases of actual section area as compared to those in air (negative value). Therefore, the reduction of area is adopted to qualitatively discuss the effects of applied potentials on wire stress corrosion cracking in this paper. SCC susceptibility decreases with the increasing of ψ_E.

In acidic solution, the wire reduction of area declines linearly with the decreasing of applied polarization potential as compared to M-shaped variation trend of reduction of area in neutral and alkaline solutions. In acidic and neutral solutions, the reduction-in-area of wire is the minimum at applied potential of E_{corr} - 500 mV as compared to the minimum at applied potential of E_{corr} + 400 mV

in alkaline solution. In applied anodic potential zone, reduction of area in acidic solution increases with the increasing of applied potential, which is due to higher anodic polarization potential, greater the anodic dissolution rate of wire surface and deeper the thickness of sample thinning. In neutral and alkaline solutions, reduction of area decreases with the increasing of applied potential, while there is a larger drop in alkaline solution. It indicates that wire SCC in acidic solution is mainly caused by hydrogen embrittlement, whereas in neutral and alkaline solutions, anodic dissolution has certain effect on stress corrosion mechanism.

In three corrosive solutions, when applied potential is E_{corr}, SCC susceptibility increases. When the applied cathodic polarization potential is E_{corr} - 250 mV, reduction of area of three samples all have the increasing trend, which indicates the steel wire can be protected in the potential range and shows good cathodic protection features. However, in cathodic potential zone, reduction of area have a trend of linear decrease with the further decrease in potential, which indicates inhibited anodic dissolution and increased cathodic hydrogen reduction reaction with the decreasing of applied cathodic potential. Meanwhile, the infiltration capacity of hydrogen in the steel increases, which reduces its mechanical strength and causes the hydrogen-induced cracking. The role of hydrogen can increase the SCC susceptibility.

Through the comparison of Fig.2 and Fig.3, it is found that in the whole applied potential range, reduction of area in neutral solution is the minimum, but tensile strength and uniform percentage elongation are larger than which in acidic and alkaline solution. That is because the corrosion effect of wire in acidic and alkaline solutions is heavy, and intense pitting and uniform corrosion cause wire tensile strength and elongation decreased. The minimum reduction of area shows that wire SCC susceptibility in neutral solution is the maximum.

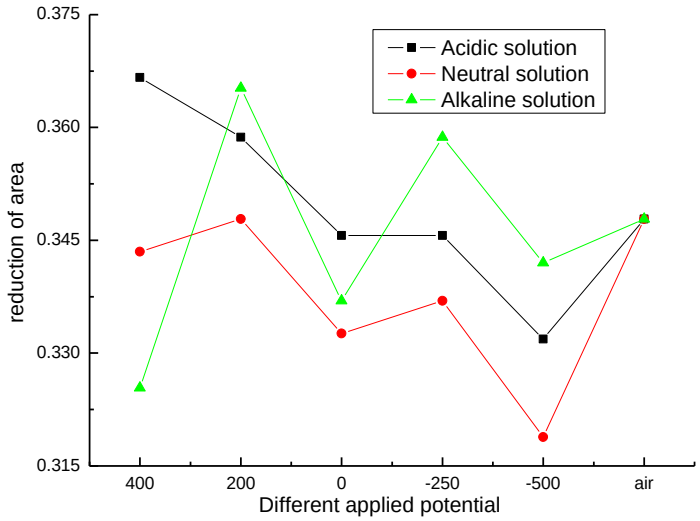

Figure 3. Reduction-in-area of steel sire under different polarization potentials in three kinds of corrosive solution

3.3 Fracture morphology analysis

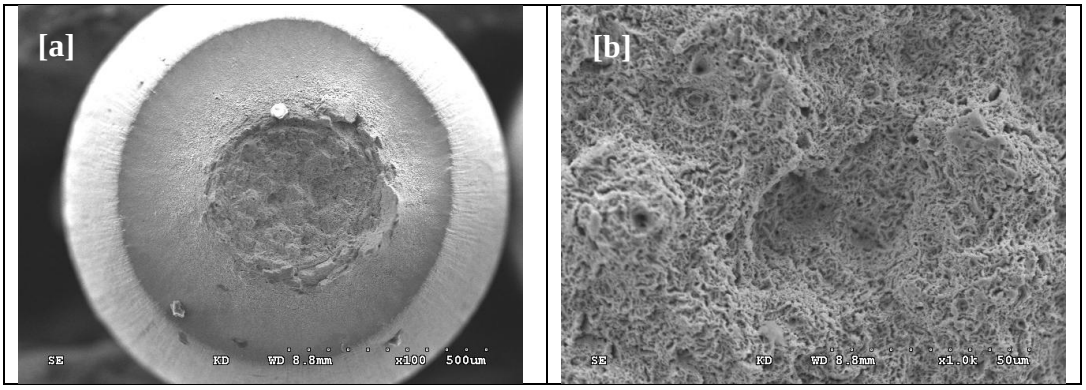

Figure 4. The macroscopic morphology and microstructure of steel wire tensile fracture in air (a) ×100; (b) ×1000

Macroscopic and microscopic fracture morphologies of steel wire in air are shown in Figure 4. It is observed that the fracture morphology shows microscope plastic porous fracture. There is no radiation zone but fiber area and shear slip. The fracture has dimple, which showed ductile fracture characteristics of larger hole pit depth and plastic deformation.

It can be seen from microscopic fracture morphology of steel wire in acidic solution (Fig.5) that the fracture has dimple morphology in the whole applied polarization potential range. However, as the applied potential decreases, the toughness characteristics reduce gradually. When the anodic polarization potential is applied, the anodic dissolution is strong. Severe general corrosion on the wire surface can not cause local crack initiation and thus SCC can not occur. There is obvious tear edge morphology in the case of E_{corr} and applied cathodic potential, which shows certain SCC susceptibility. This demonstrates that the strong anodic dissolution only causes general corrosion but not SCC in anodic polarization of acidic solution. However, in self-corrosion zone and cathodic polarization zone, the SCC susceptibility is strengthened with the decreasing of applied potential, which is consistent with the results of Figure 3.

Figure 6 shows the microscopic fracture morphologies of steel wires in neutral solution. It can be observed that there is dimple morphology in the whole. The most obvious dimple features and worst SCC susceptibility are present when applying ΔE equal to 200 mV and -250 mV. In the process of applying anodic polarization potential, anodic dissolution has certain effect on stress corrosion mechanism. Local anodic dissolution forms pits crack. When the anodic dissolution of crack tip continuously occurs, the precipitation of hydrogen is accompanied. The hydrogen is easy to cause hydrogen-induced delay in fracture. Higher anodic potential induces larger amount of precipitated hydrogen, easier hydrogen embrittlement and stronger SCC susceptibility. Because the reduction of area in anodic polarization zone decreases with the increasing of potential, we believe hydrogen plays a dominant role in the process of wire SCC in neutral solution.

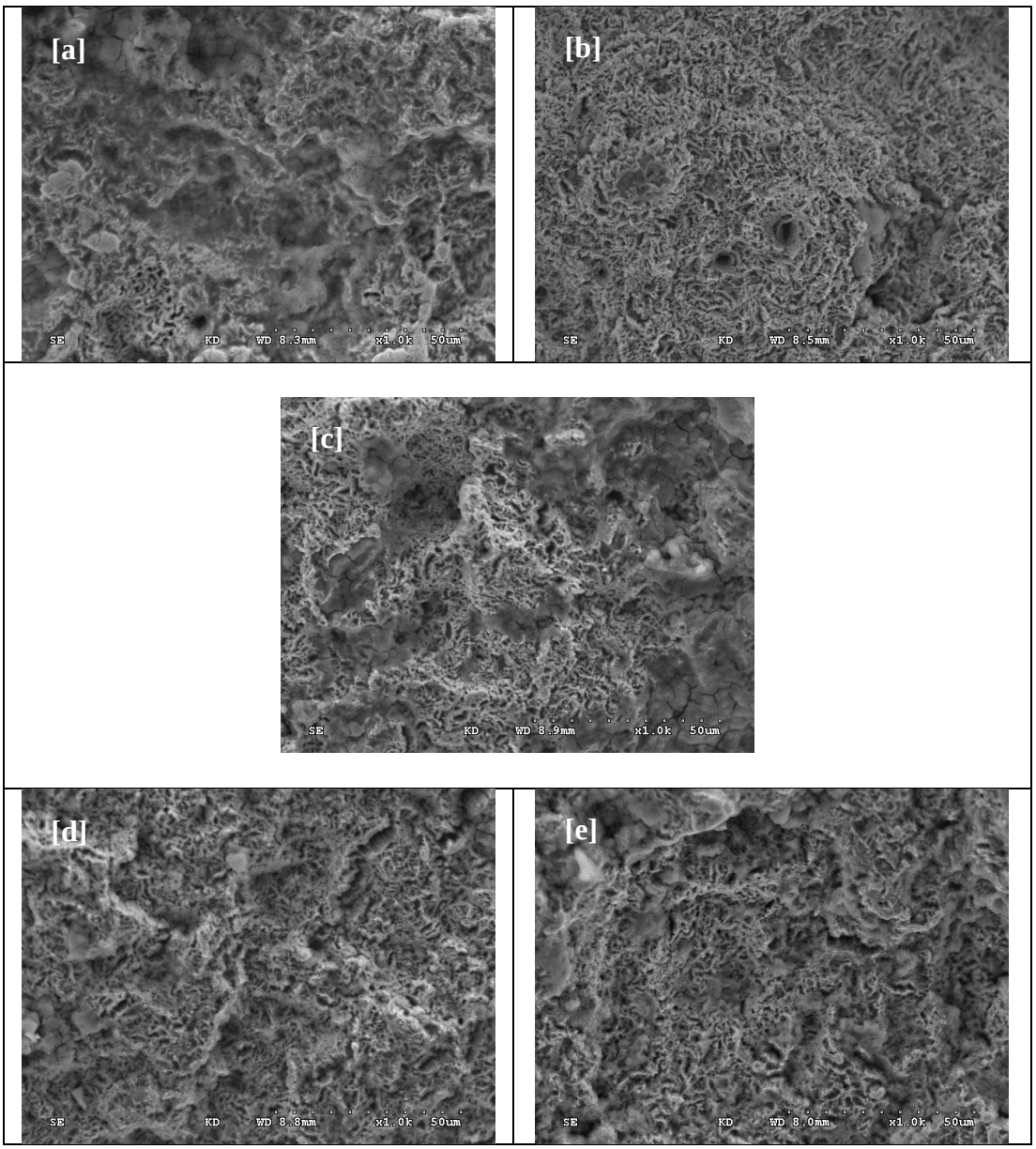

Figure 5. Micro-fracture morphology of the wire in acidic solution (a) E_{corr} + 400 mV; (b) E_{corr} + 200 mV; (c) E_{corr} + 0 mV; (d) E_{corr} - 250 mV; (e) E_{corr} - 500 mV

Figure 7 shows the microscopic fracture morphologies of steel wires in alkaline solution. The fracture section still mainly presents the dimple morphology. When applied polarization potentialΔE related to E_{corr} is 400 mV and -500 mV, the local fracture shows brittle cleavage section. When applied potential in anodic polarization zone is 400 mV, the sample surface can easily form deep pits due to larger anodic potential, which induces crack nucleation and propagation. Therefore, the fracture has a few brittle fracture features. However, the cathodic polarization can inhibit the anodic dissolution of steel wires and thus slow down the corrosion of the crack tip. With the further negatively shift of

cathodic polarization potential, SCC susceptibility further increases due to strong hydrogen evolution reaction and brittleness increases.

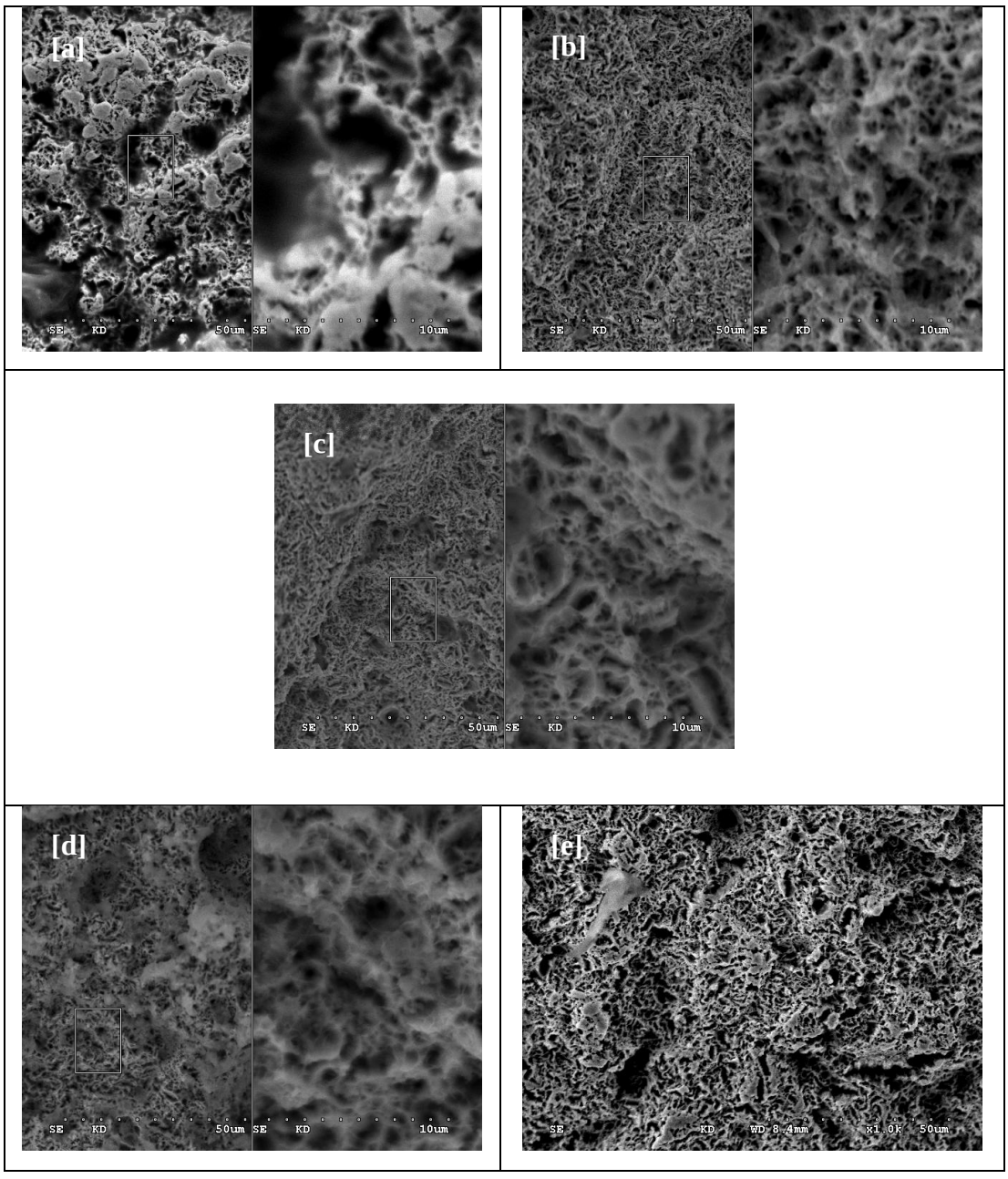

Figure 6. Micro-fracture morphology of steel wires in neutral solution (a) E_{corr} + 400 mV; (b) E_{corr} + 200 mV; (c) E_{corr} + 0 mV; (d) E_{corr} - 250 mV; (e) E_{corr} - 500 mV

In self-corrosion zone, SCC susceptibility is larger attributed to the common action of anodic dissolution of crack tips and hydrogen evolution reaction of non-crack tips, which induces weakened dimple characteristics and local brittle cleavage morphology.

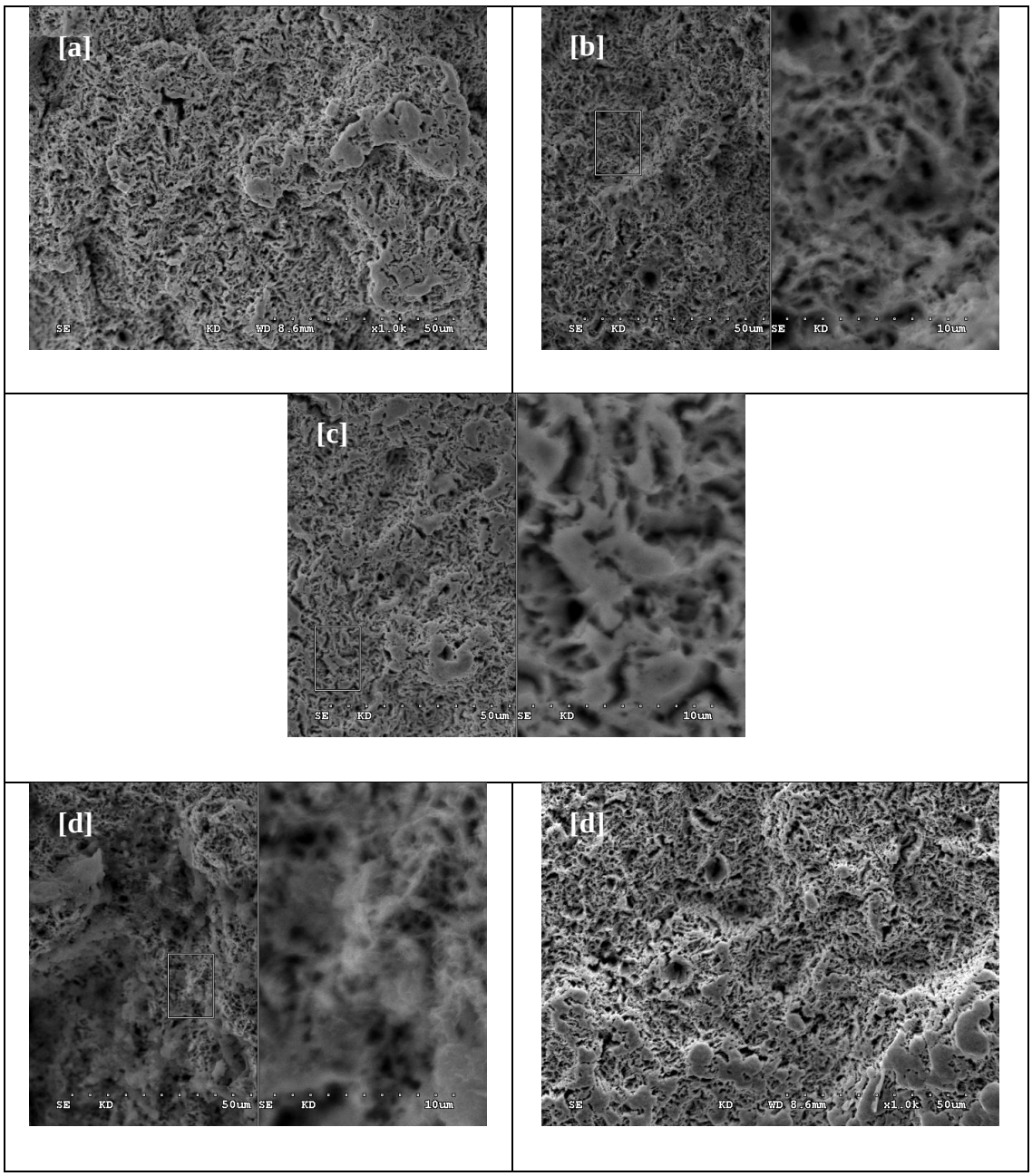

Figure 7. Micro-facture morphology of steel wires in alkaline aolution (a) E_{corr} + 400 mV; (b) E_{corr} + 200 mV; (c) E_{corr} + 0 mV; (d) E_{corr} - 250 mV; (e) E_{corr} - 500 mV

3.4 The measurement of polarization curves

According to the Parkins theory [33], differences of electrochemical corrosion in crack tip and non-crack tip region can be determined by fast and slow scanning polarization curves. Then the SCC possibility is determined through fast and slow differences of current density under certain boundary conditions.

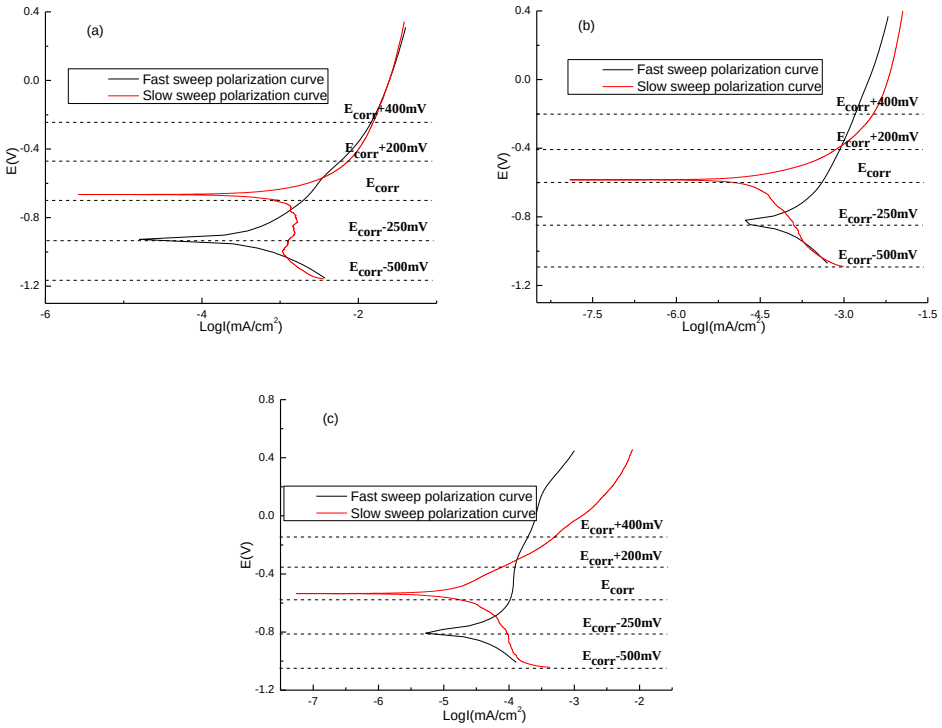

Figure 8. Fast and slow polarization curves in different corrosive solution (a) acidic solution; (b) neutral solution; (c) alkaline solution

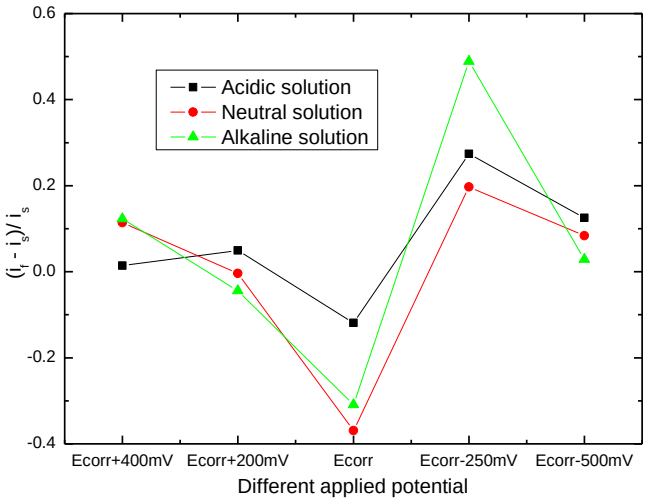

Figure 9. The difference of wire current density at fast and slow rate under different polarization potentials in three solutions.

This paper presents electrochemical polarization curves at fast and slow rates in different corrosive mediums simulated trickling waters and differences of current density $(i_f - i_s)/ i_s$ at fast and

slow rate under different conditions of constant potential polarization. (Parameters of i_f and i_s are current density at fast and slow rates, respectively).

Figure 8 shows electrochemical polarization curves of steel wires at fast and slow rates in three corrosive solutions. Figure 9 exhibits the differences of scanning current density at fast and slow rates under different polarization potentials in three corrosive solutions. By comparisons of Figs. 8 and 9, it is found that when potential of 400 mV related to open circuit potential in three corrosive solutions is applied, the crack tip (no corrosion product film on the surface, fast polarization curve) and non-crack tip (corrosion product film, slow polarization curve) are both anodic polarization zones. Meanwhile, they have the same electrode process with the metal dissolution reaction as written in Eq. (1).

$$Fe\text{-}2e \rightarrow Fe^{2+} \qquad 1$$

The difference in anodic current density in acidic solution is the smallest and the SCC susceptibility caused by anodic dissolution is the weakest, which indicates the wires are less prone to occur stress corrosion cracking. Larger difference in anodic current density in neutral and alkaline solutions reveals the larger SCC susceptibility is controlled by anodic dissolution under the applied potential. When potential of 200 mV related to E_{corr} is applied, the values of $(i_f - i_s)/ i_s$ in three solutions are all close to zero, which shows smaller SCC tendency of steel wires. However, the polarization process of crack tip in alkaline solution is opposite to that of non-crack tip. Non-crack tip shows hydrogen evolution reaction, which indicates its SCC mechanism is controlled by both anodic dissolution and hydrogen embrittlement. The present study applies all-soak solution, and all specimens are in hypoxic state. Therefore, the cathodic reaction equation is given by

$$H_2O+e \rightarrow OH^-+H \qquad 2$$

For three corrosive solutions, in self-corrosion zone, the crack tip and non-crack tip are anodic polarization zone and cathodic polarization zone, respectively, and the current density difference is negative, which indicates the opposite polarization process. In addition, metal dissolution, and hydrogen evolution reaction occurs in the crack tip and non-crack tip. The current density difference is large. Under this applied potential, the SCC mechanism is controlled by both anodic dissolution and hydrogen embrittlement, and the SCC tendency is also larger. Eq. (3) shows the process of cathodic reaction in acidic solutions as compared to Eq. (2) in neutral and alkaline solutions. Because $HCO3^-$ ions in neutral solution exist, hydrogen evolution reaction also occurs as given in Eq. (4).

$$H^+ + e \rightarrow H \qquad 3$$

$$HCO_3^- + e \rightarrow CO_3^{2-} + H \qquad 4$$

When the applied potential related to E_{corr} is -250 mV, the variation from anodic polarization zone to cathodic polarization zone in the crack tip and positive current density difference with the applied potential shifting negatively indicate the same polarization processes and occurrences of hydrogen evolution reaction in the crack tip and non-crack tip. Because the cathodic current in the crack tip is smaller, the value of $(i_f - i_s)/ i_s$ is larger. Under this applied polarization potential, the SCC mechanism of steel wires is mainly controlled by hydrogen embrittlement. However, the small cathodic current in crack tip and low amount of hydrogen evolution induces weaker SCC susceptibility.

With the applied potential further shifting negatively, when ΔE of -500 mV, the value of $(i_f - i_s)/ i_s$ declines significantly and is close to zero. Under the strong cathodic polarization, hydrogen evolution makes it difficult to form the oxide film. Therefore, the differences between electrode reaction in crack tip and non-crack tip zones are very small, i.e. both being hydrogen evolution reaction. Then the SCC mechanism of steel wires is induced by hydrogen embrittlement completely. Severe hydrogen evolution reaction causes increased hydrogen content and enhanced SCC susceptibility.

4. CONCLUSIONS

(1) Steel wires in three corrosive mediums simulated trickling water all present SCC susceptibility. In neutral solution, tensile steel wires exhibit the minimum reduction of area and maximum SCC susceptibility.

(2) The SSRT tensile fracture morphologies of steel wires in air and in three corrosive solutions are mainly the dimple morphologies. The SCC-sensitive area presents a small amount of brittle fracture characteristics. Fraction sections all show obvious tear prism appearances when applying cathodic potential in different solutions.

(3) When the strong anodic polarization potential is applied, the steel wire does not occur SCC in acidic solution, and the SCC is controlled by anodic dissolution in neutral and alkaline solutions. With the decreasing of applied anodic potential, SCC mechanism in alkaline solution is controlled by anodic dissolution and hydrogen embrittlement. In the self-corrosion zone, SCC mechanisms of steel wires in three solutions are all controlled by anodic dissolution and hydrogen embrittlement revealing stronger SCC susceptibility. When the cathodic polarization potential is applied, SCC mechanisms in three corrosive solutions are all controlled by hydrogen embrittlement. With the increasing of applied cathodic potential, the cathodic current increases in the crack tip. Strong hydrogen evolution reaction enhances the SCC susceptibility.

ACKNOWLEDGEMENTS

This research was financed by Jiangsu College Postgraduate Research Innovation Plan Project of 2012 (CXZZ12_0927).

References

1. T. P. Hoar, J. G. Hinse, *J. Iron. Steel Inst*., 182 (1956) 124.
2. P. R. Rhodes, *Corro.*, 25 (1969) 462.
3. T. P. Hoar, J. C. Scully, *J. Electrochem. Soc*., 111 (1964) 348.
4. E. N. Pugh, In: Scully J C ed., The Theory of Stress Corrosion Cracking in Alloys, Brussels: NATO. 1971: 21
5. R. W. Staehle, In: Scully J C ed., The Theory of Stress Corrosion Cracking in Alloys, Brussels: NATO. 1971: 223.
6. H. H. Uhlig, In: Rhodined T N ed., Physical Metallurgy of Stress Corrosion Fracture, New York: Interscience, 1959: 1.
7. N. A. Nielsen, In: Rhodined T N ed., Physical Metallurgy of Stress Corrosion Fracture, New York: Interscience, 1959: 341.
8. Galvele, R. Jose, *Corro. Sci*., 27 (1987) 1.
9. D. A. Jones, *Metallurgic. Trans*., 16A (1985) 1133.
10. C. N. Cao, China National Materials Symposium, Wu Han, (1988) 238.
11. C. Manfredi, J. L. Otegui, *Eng. Failure. Anal*., 9 (2002) 495.
12. S. Yamazaki, Z. P. Lu, Y. Ito, Y. Takeda, T. Shoji, *Corro. Sci.*, 50 (2008) 835.
13. J. B. Li, X. Hou, M. S. Zheng, J. W. Zhu, *Int. J. Electrochem. Sci.*, 2 (2007) 607.
14. P. L. Andress, M. M. Morra, J. Hickling, K. S. Ahluwalia, J. A. Wilson, 13th Int Symp Environmental Degradation of Materials in Nuclear Power Systems-Water Reactors. British Columbia: CNS, Aug 13-23, 2007.
15. M. Olszta, D. Edwards, S. Bruemmer, ICG-EAC 2008 Conference. Bastad Sweden, Apr 20-25, 2008.
16. P. L. Andresen, J. Hickling, A. Ahluwalia, J. Wilson, *Corrosion*, 64 (2008) 707
17. A.Torres-lslas, J. G. Gonzalez-Rodriguez, *Int. J. Electrochem. Sci.*, 4 (2009) 640.
18. Torres-lslas, J. G. Gonzalez-Rodriguez, J. Uruchurtu, S, Serna, *Corr. Sc*i., 50 (2008) 2931.
19. Y. Z. Jia, J. Q. Wang, E. H. Han, W. Ke, *J. Mater. Sci. Technol.*, 27 (2011) 1039.
20. A.Contreras, S. L. Hernandez, R. Orozco-Cruz, R, Galvan-Martinez, *Materials & Design*, 35 (2012) 281.
21. Z. Y. Liu, G. L. Zhai, C. W. Du, X. G. Li, ACTA *Metallurgica. Sinica*., 44 (2008) 209.
22. Z. Y. Liu, X. G. Li, C. W. Du, Y. F. Cheng, *Corro. Sci*., 51 (2009) 2863
23. R. N. Parkins, J. A. Beavers, *Corro*., 59 (2003) 258.
24. Manfredi, J. L. Otegui, *Eng. Failure Anal*., 9 (2002) 495.
25. J. Q. Wang, A. Atrens, *Corr. Sci*., 45 (2003) 2199.
26. R. Chu, W. Chen, S. H. Wang, et al, *Corro*., 60 (2004) 275.
27. T. Lu, J. L. Luo, *Corro*., 62 (2006) 129.
28. W. Chen, F. King, E. Vokes, *Corro*., 58 (2002) 267.
29. Y. L. Huang, C. N. Cao, H. C. Lin, M. Lu, ACTA *Metallurgica. Sinica*., 29 (1993) 212.
30. W. E. Ruther, W. K. Soppet, *Corro*., 40 (1984) 518.
31. P. Berge, J. R. Donati, *Nuc.l Technol*., 55 (1981) 88.
32. H. Guo, G. F. Li, X. Cai, W. Yang, ACTA *Metallurgica. Sinica*., 40 (2004) 967.
33. R. N. Parkins, *Corr. Sci*., 20 (1980) 147.